Asian Journal of Chemistry; Vol. 38, No. 4 (2026), 1065-1072
ASIAN JOURNAL OF CHEMISTRY
https://doi.org/10.14233/ajchem.2026.35421

Homopolymer and Copolymer of Dodecyl Acrylate Incorporated with *Elsholtzia blanda*–Chitosan-Mediated CuO Nanoparticles: A Study on Their Multifunctional Additive Performance in Lubricating Oils

LEIYAMI AHUNGSHI[1], ATHISA ROSELYN MAHEO[2] and MAINUL HOQUE[3,*]

[1]Department of Chemistry, Bodoland University, Kokrajhar-783 370, India
[2]Department of Chemistry, Auxilium College, Udalguri-784509, India
[3]Department of Chemistry, Kokrajhar University, Kokrajhar-783370, India

*Corresponding author: E-mail: mainulkgc@gmail.com

Received: 8 December 2025 *Accepted*: 13 March 2026 *Published online*: 8 April 2026 AJC-22330

Polymer nanocomposite has attracted a lot of attention since it outperforms traditional polymers in the lubricant industry. In this study, chitosan and the aqueous leaf extract of the fragrant medicinal plant *Elsholtzia blanda* were used to synthesise copper oxide nanoparticles. Several analytical methods, such as X-ray diffraction (XRD), field emission scanning electron microscopy (FE-SEM), high-resolution transmission electron microscopy (HRTEM) and selected area electron diffraction (SAED), were used to characterize the produced *E. blanda*-chitosan-mediated copper oxide nanoparticles (COEC). Several instrumental studies were used to describe the polymer/COEC nanocomposites that were created by incorporating these COEC nanoparticles at different concentrations into olive oil-based polymers. In accordance with normal ASTM methods, the nanocomposites were blended with mineral-based oil in varying amounts to evaluate their effectiveness as pour point depressants, viscosity index improvers and anti-wear additives. The results showed that adding more nanocomposite material greatly improved the formulated oil's overall lubricating capabilities.

Keywords: Olive oil, Copper oxide nanoparticles, Free radical polymerisation, Anti-wear properties.

INTRODUCTION

Recent efforts have focused on developing environmentally friendly lubricants that enhance efficiency, extend machine lifespan, reduce operational costs and improve energy conservation. These lubricants form a protective film on contact surfaces, minimizing friction during tribochemical interactions. The use of oil-soluble additives as efficient friction-reducing and anti-wear agents has been the subject of much lubrication engineering study over the last few decades [1,2]. The usage of these compounds, however, exacerbates environmental problems such as pollution, toxicity and difficulties with the waste management. Nanomaterials are considered promising environmentally friendly lubricant additives and have attracted considerable research interest due to their diverse industrial applications. In this context, nanolubricants have emerged as a rapidly growing field, offering new opportunities for improving lubrication performance and advancing the lubricant industry [3-5].

To improve the lubricating oils' tribological performance, nanoparticles have been introduced [6]. The efficacy of different inorganic origin nanoparticles as additives in different kinds of lubricating oils as wear-reducing and friction reducing agents has been the subject of numerous studies in recent years [7-9]. The primary advantage of nanoparticles lies in their nanometer-scale size, which makes them highly suitable for effectively filling friction interfaces. This allows them to perform a variety of tasks, including acting as friction modifiers, anti-wear and extreme-pressure additives. Nanoparticles can adhere to micro-defects on friction surfaces and exhibit a self-repairing effect, facilitated by their low melting point and high chemical reactivity [10]. The size, shape and concentration of the nanoparticle all affect its ability to reduce friction and prevent wear. These nanoparticles are usually between 3 and 130 nm in size [11-13].

Nanoparticles have emerged as effective alternatives to conventional lubricant additives due to their superior tribological properties and eco-friendly nature, particularly under

This is an open access journal, and articles are distributed under the terms of the Attribution 4.0 International (CC BY 4.0) License. This license lets others distribute, remix, tweak, and build upon your work, even commercially, as long as they credit the author for the original creation. You must give appropriate credit, provide a link to the license, and indicate if changes were made.

conditions of high load, rapid sliding and severe friction [14-17]. Furthermore, inorganic nanoparticles play a transformative role in lubrication by serving as advanced additives that overcome the limitations of traditional lubricant formulations, especially under high-load and elevated temperature conditions. For instance, the anti-wear properties of paraffin oil were significantly improved by the inclusion of MoS_2 nanoparticles [18-20]. CuO nanoparticles have demonstrate an excellent anti-wear and reduced friction capabilities [21], while CeO_2 and TiO_2 nanoparticles has the ability to decrease the friction and minimize wear when mixed with lubricating oil [22,23]. It is also found that CeO_2 nanoparticles can prevent particle agglomeration and enhance the stability of nanoparticles within an organic liquid medium [22].

The lubricating efficacy of copper nanoparticle additives is greatly influenced by their size and concentration. The reaction film formed by the surface modification agent, along with the copper deposition layer generated during friction, acts synergistically to enhance anti-wear properties, reduce friction and improve load-bearing capacity [11,24]. By filling in surface fissures and crevices, the lubricant with Fe_3O_4 nanoparticles forms a protective layer that sticks to the steel friction pairs. This effect is probably caused by tribochemical processes taking place on the metal surface as well as magnetic interactions between the lubricant and the friction surface [25,26]. Even though a lot of research has been done on lubricant additives based on nanoparticles, the majority of studies emphasize single-function performance and concentrate on the direct dispersion of nanoparticles into base oils to reduce wear and friction. There is limited exploration of multifunctional additive systems capable of enhancing pour point (PP), viscosity index (VI) and anti-wear performance simultaneously. Most reported polyacrylate–nanoparticle systems with CuO additives rely on the synthetic polymers or straightforward physical mixing methods. While vegetable oil–based polymers have been widely applied as viscosity modifiers, their combination with nanoparticle systems has received limited attention. In particular, the integration of green-synthesized CuO nanoparticles into olive oil–based polymer backbones to develop multifunctional nanocomposite additives remains largely unexplored. Thus, keeping in mind these facts, the present study designs olive oil–based homopolymer and copolymer matrices with direct incorporation of plant-mediated CuO nanoparticles into the polymer backbone. This approach enables the simultaneous enhancement of pour point (PP), anti-wear performance and viscosity index (VI) within a single sustainable system. Such an integrated bio-based nanocomposite strategy represents a clear advancement over conventional CuO-based and polyacrylate–nanoparticle systems, which largely rely on separate or physically blended components.

EXPERIMENTAL

Olive oil containing 86% unsaturated and 15% saturated fatty components [27] was procured from a nearby market. Benzoyl peroxide (98% purity), was purchased from LOBA Chemie, India and purified through recrystallisation with chloroform–methanol solvent mixture prior to application. The base oil SN150 was obtained from the Indian Oil Corporation Limited (IOCL), Dhakuria, India. Copper(II) sulphate pentahydrate ($CuSO_4·5H_2O$), sodium hydroxide (NaOH) and acetic acid (CH_3COOH) were procured from Spectrum Reagents and Chemicals Pvt. Ltd., Edayar, Cochin, India while chitosan was obtained from Sisco Research Laboratories Pvt. Ltd. Leaves of *Elsholtzia blanda* were collected from Manipur, India and their taxonomic identification was confirmed by Department of Botany, D.G. Vaishnav College, Chennai, India.

Synthesis of homopolymer and copolymer: Copolymer was synthesised using olive oil and dodecyl acrylate monomers in different proportional ratios. Benzoyl peroxide (BZP) served as the initiator for the reaction, which was conducted solvent-free *via* free radical polymerisation. A three-necked round-bottom flask with a condenser, thermometer, magnetic stirrer and nitrogen intake was used to carry out the polymerisation process. First, a set quantity of acrylate monomer and olive oil was heated to 90 ºC for 0.5 h. The reaction mixture was then kept at the same temperature for 6 h after BZP was added at a concentration of 1% w/w in relation to the total monomer content. Following completion, the mixture was poured into cold methanol while being constantly stirred to stop the reaction and cause polymer precipitation. After dissolving the crude polymer in hexane, it was re-precipitated with cold methanol to purify it. The purified polymer was then vacuum-dried at 50 ºC. The same synthesis and purification procedures were applied for the preparation of the olive oil homopolymer [27,28]. The percentage yield of copolymer and homopolymer was 89.5 and 82.6 respectively.

Preparation of CuO nanoparticle using chitosen and plant extract: Copper oxide nanoparticles mediated by *E. blanda*–chitosan (COEC) were synthesised using a modified protocol [29,30]. In brief, chitosan solution was prepared by dissolving 1.5 g of chitosan in 100 mL of 1.5% acetic acid at 60 ºC. Separately, 1.25 g of $CuSO_4·5H_2O$ was dissolved in 100 mL of double-distilled water. Then, a portion (60 mL) of this solution was mixed with 20 mL of *E. blanda* aqueous extract and stirred for 30 min. Subsequently, 20 mL of 0.6 M NaOH was added dropwise until the pH reached ~9. Thereafter, 20 mL of chitosan solution was added gradually and the mixture was further stirred at 70 ºC for 3 h. A noticeable colour change from blue to green and finally to greenish-black confirmed the formation of CuO nanoparticles. The reaction mixture was cooled, filtered and repeatedly washed with double distilled water. The obtained nanoparticles were dried at 80 ºC, yielding 80.5% and were further subjected to characterisation.

Synthesis of polymer-*Elsholtzia blanda*-chitosan mediated copper oxide nanocomposites (COEC): The polymer -COEC nanocomposites were prepared by blending the synthesised homopolymer and copolymer with COEC nanoparticles in a toluene medium. For preparation, 5 g of both the polymers were dissolved in toluene and specific quantities of COEC nanoparticles (0.01, 0.02, 0.03 and 0.04 g) as shown in Table-1, were incorporated under ultrasonic agitation while maintaining constant stirring. A semi-solid polymer–nanocomposites material was formed when the resultant homogeneous suspension was put onto a glass plate and allowed to evaporate naturally. The obtained nanocomposites were subsequently subjected to characterisation [31].

TABLE-1
DESIGNATION AND COMPOSITION OF POLYMER–COEC NANOCOMPOSITES

Designation	Polymer (g)	Nanoparticle (g)
P-1/P-2	5.00	0.00
P-1A/P-2A	4.99	0.01
P-1B/P-2B	4.98	0.02
P-1C/P-2C	4.97	0.03
P-1D/P-2D	4.96	0.04

Characterization: FTIR and NMR spectroscopy were used to characterize the produced polymers and their composites spectrally. Using 0.1 mm KBr cells and a Shimadzu FT-IR 8300 spectrometer, FTIR spectra were acquired at room temperature in the 4000-400 cm^{-1} range. A Bruker Avance 400 MHz FT- NMR spectrometer with a 5 mm BBO probe and $CDCl_3$ as the solvent was used to record the NMR spectra, with TMS acting as the internal reference standard. Using an alumina ceramic crucible in air, a thermogravimetric analyzer (Thermal Analysis System TGA-2, Make: Mettler Toledo, Temperature accuracy ±1 K) was used to determine the thermal stabilities of the homopolymer, copolymer and its nanocomposite. A heating rate of 10 ºC/min was maintained and the percentage weight loss (PWL) of the samples was recorded as the temperature increased. X-ray diffraction (XRD) analysis was used to analyze the CuO nanoparticles and their composite materials over a 2θ range of 10º to 90º using a Bruker D8 Advance diffractometer (Germany) fitted with a 2.2 kW Cu-anode ceramic X-ray source. Surface morphology and elemental composition of the samples were analyzed using field emission scanning electron microscopy (FESEM). Further structural characterization, including particle shape and grain size, was performed using high-resolution transmission electron microscopy (HRTEM) at an accelerating voltage of 200 kV, along with selected area electron diffraction (SAED) analysis.

Determination of average molecular weight by GPC method: A size exclusion chromatography–gel permeation chromatography (SEC-GPC) system was used to measure the synthesised polymers' number-average molecular weight (Mn), weight-average molecular weight (Mw) and polydispersity index (PDI). A 2414 refractive index detector, a Waters 515 HPLC pump, a 717 Plus autosampler and a 2489 UV/Visible detector made up the setup, which was calibrated using polystyrene standards. The analysis was carried out at a constant temperature of 30 ºC using HPLC-grade THF as the mobile phase at a flow rate of 1.0 mL/min [32].

Determination of viscosity index: The viscosity index (VI) represents the extent to which the viscosity of a base oil changes with temperature. Higher VI values indicate improved viscosity stability, whereas lower values reflect greater temperature sensitivity. The effectiveness of the polymeric additive as a viscosity modifier was evaluated by determining the VI of paraffinic base oil at different additive concentrations, calculated according to ASTM D2270 using the method reported by Tanveer & Prasad [33].

Determination of pour point (PP): At low temperatures, lubricants can lose fluidity due to wax crystallization, forming a gel-like structure. The pour point (PP) represents the temperature at which this occurs. The effectiveness of polymeric additives in reducing PP was evaluated using a Cloud and Pour Point Tester (Model WIL-471, India) following ASTM D97, with additive concentrations between 1-5% (w/w).

Determination of anti-wear property: Using a Four-Ball Wear Tester (FBWT) in accordance with ASTM D4172-94, the anti-wear performance of lubricant compositions comprising additives at concentrations ranging from 1% to 5% was evaluated. In order to measure the wear scar diameter (WSD), a load of 392 N (40 kg) was applied for 30 min at a temperature of 75 ºC. The steel balls of 12.7 mm diameter were used in the test, and the rotational speed was maintained at 1200 rpm [34].

RESULTS AND DISCUSSION

Spectroscopic studies: The FTIR spectrum of the polymer (Fig. 1a) shows a characteristic ester carbonyl (C=O) stretching band at 1749 cm^{-1}. In the polymer/nanocomposite system (Fig. 1b), this peak shift slightly to 1744 cm^{-1}, indicating possible interactions between the COEC nanoparticles and the polymer matrix. The peaks at 1471, 1465, 1272 and 1277 cm^{-1} correspond to the asymmetric and symmetric bending vibrations of C–H bonds in $–CH_3$ and $–CH_2$ groups. Bands observed between 1166 and 1161 cm^{-1} are assigned to C–O stretching of ester groups, while peaks near 716 and 708 cm^{-1} represent the C–H bending of paraffinic chains. Moreover, broad bands at 2931, 2846, 2924 and 2856 cm^{-1} are attributed to the C–H stretching vibrations of $–CH_2$ groups. The absence of peaks in the olefinic region confirms the successful formation of the polymer structure.

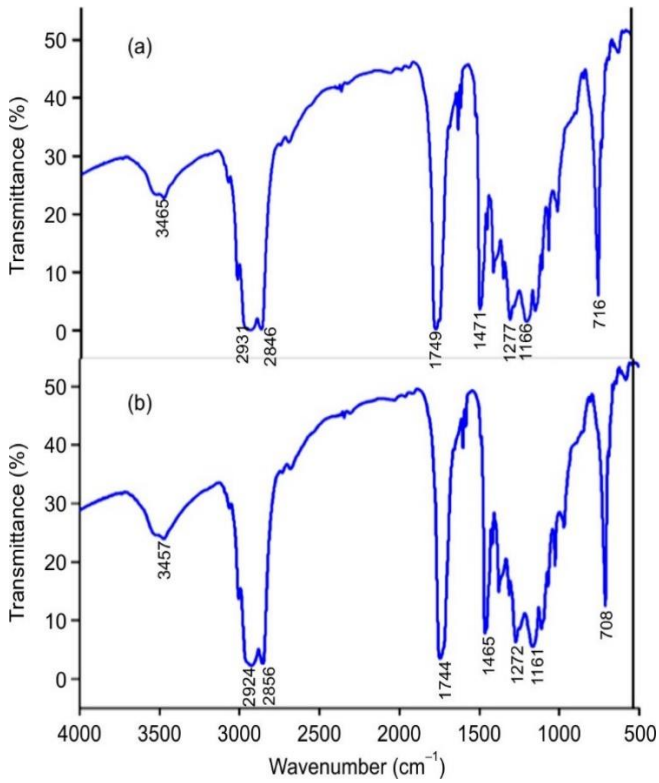

Fig. 1. FT-IR spectra of (a) homopolymer/COEC nanocomposite (b) copolymer/COEC nanocomposite

Fig. 2 presents the ^{1}H NMR spectra of the polymer/-COEC nanocomposites, where spectrum (a) corresponds to the homopolymer nanocomposite and spectrum (b) to the co-polymer nanocomposite. Spectrum (a) shows a broad singlet between δ 2.33 and 4.29 ppm, which is attributed to the polymer's $–OCH_2$ protons. The methyl protons of the polymer backbone are visible at 0.80 ppm and the absence of any signal in the δ 5.55-7.0 ppm area suggests the absence of vinylic protons. The $–OCH_2$ proton signal can be seen at δ 2.29 ppm in spectrum (b). The α-hydrogens next to the ester carbonyl group are represented by a peak at δ 2.00 ppm, whereas the methyl and methylene protons are found between 0.90 and 1.61 ppm. The copolymer's lack of vinylic protons is confirmed by the absence of peaks in the δ 5.55-7.0 ppm region, much similar in the homopolymer.

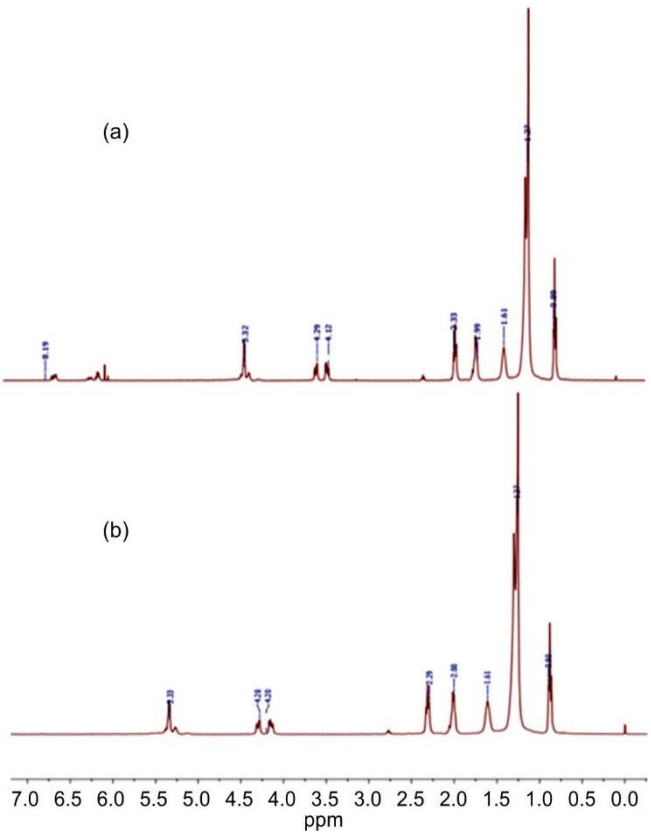

Fig. 2. ^{1}H NMR spectra of (a) homopolymer/COEC nanocomposite and (b) copolymer/COEC nanocomposite

Fig. 3 shows the ^{13}C NMR spectra for the homopolymer and copolymer nanocomposites, designated as (a) and (b). In spectrum (a), carbonyl carbon is observed at 129.99 ppm, while other sp^3 carbons appear between δ 68.92 and 13.86 ppm. In the copolymer spectrum (b), the carbonyl carbon slightly moves to 123.39 ppm. The sp^3 carbons of the alkyl chains in the nanocomposites are represented by signals that appeared between δ 14.05 and 31.95 ppm. The reduced intensity of NMR signals in the polymer composites can be attributed to interference from microwave frequencies generated by magnetic components. The appearance of an additional peak is likely due to the presence of minor impurities. These observations are in agreement with the reported findings [35].

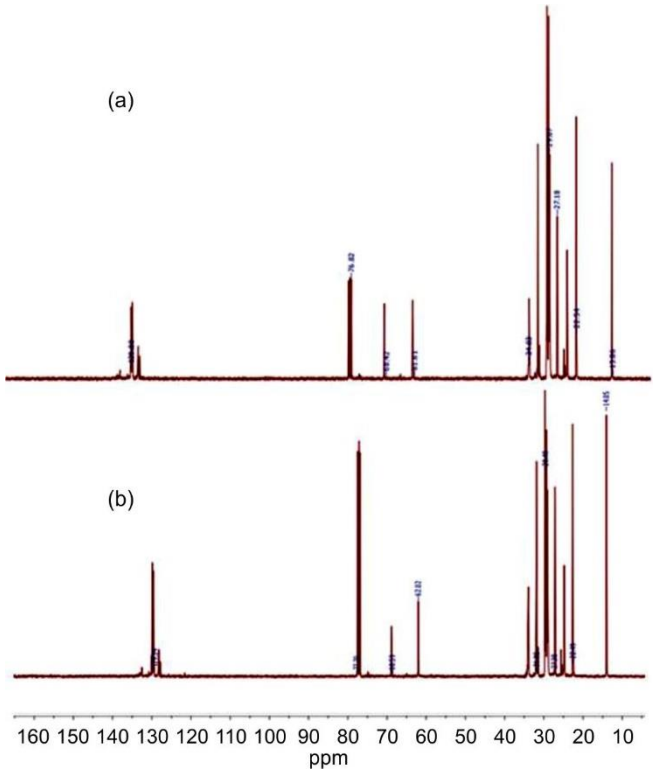

Fig. 3. ^{13}C NMR spectra of (a) homopolymer/COEC nanocomposite and (b) copolymer/COEC nanocomposite

Molecular weight data analysis: To ascertain the number-average (Mn) and weight-average (Mw) molecular weights of the synthesised polymers, HPLC-grade THF was used in gel permeation chromatography (GPC) conducted at room temperature as shown in Table-2. The results indicate that between the two polymer samples, P-2 possesses the higher molecular weight and higher PDI value. Lubricant performance is greatly influenced by the molecular weight distribution, which is represented by the polydispersity index (PDI). By preserving thickening at high temperatures and fluidity at low temperatures, a moderate PDI supports an effective improvement in the viscosity index (VI) by reflecting a balanced chain length distribution. Shear stability, anti-wear behaviour and homogeneous film formation are all improved by a comparatively narrow distribution. Stable viscosity modification and enhanced load-bearing performance in lubricant applications are facilitated by the acquired PDI values, which show regulated polymerisation and an appropriate chain structure.

TABLE-2
MOLECULAR WEIGHT OF THE PREPARED POLYMER (Mn, Mw AND PDI VALUE)

Sample code	Mn	Mw	PDI
P-1	12671	13568	1.07
P-2	16251	19869	1.22

Note: P-1: 100% oil, P-2: 90% oil + 10% DDA, Mn: number average molecular weight, Mw: weight average molecular weight, PDI: polydispersity index, Oil: olive oil

Thermal studies: Thermogravimetric analysis of the homopolymer/COEC nanocomposite (a) and copolymer/COEC

nanocomposite (b), demonstrates distinct degradation behaviour as depicted in Fig. 4. Due to the removal of moisture, both samples show a slight initial weight loss at low temperatures. At intermediate temperatures, there is a significant breakdown of the polymer backbone. Compared to (a), sample (b) shows a slower degradation rate and higher residual char formation, indicating superior thermal stability and oxidation resistance. Stronger interfacial contacts between the nanoparticles and the copolymer matrix, better dispersion and the intrinsic structural stability of the copolymer backbone are all responsible for the increased stability of the copolymer/COEC nanocomposite. Furthermore, the thermal stability observed in TGA aligns with the GPC results, as a controlled molecular weight distribution enhances resistance to thermal degradation. The combined GPC and TGA findings confirm that the synthesized polymers and their CuO nanocomposites possess suitable molecular structure and thermal stability for the multifunctional lubricant applications.

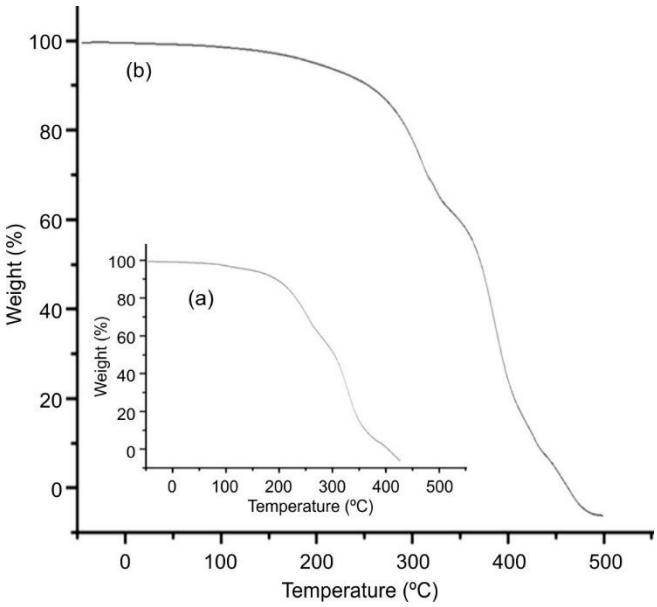

Fig. 4. TGA of (a) homopolymer/COEC nanocomposite and (b) copolymer/COEC nanocomposite

XRD studies: The XRD technique was used to investigate the crystal structure of the prepared COEC nanoparticles and the results are displayed in Fig. 5. The data was acquired spanning the 2θ range of 10º to 90º. The four most noticeable peaks corresponding to (110), (111), (202), (113), (311) and (220) were 35.5º, 38.7º, 48.8º, 61.5º, 66.4º and 68.2º at 2θ values for CuO. The face-centered cubic (fcc) structure of the crystallites is indicated by the peaks and the corresponding nanoparticle values. These peaks are very similar to the findings reported earlier [36]. The presence of contaminants may be indicated by additional peaks in the pattern.

Morphological studies: The surface shape and size generated of COEC nanoparticles were examined using field emission–scanning electron microscopy (FE-SEM). As illustrated in Fig. 6a, the FE-SEM images of COEC revealed predominantly short rod-shaped structures, along with some spherical particles. The particle size of COEC was found to range between 30.76 nm and 69.08 nm.

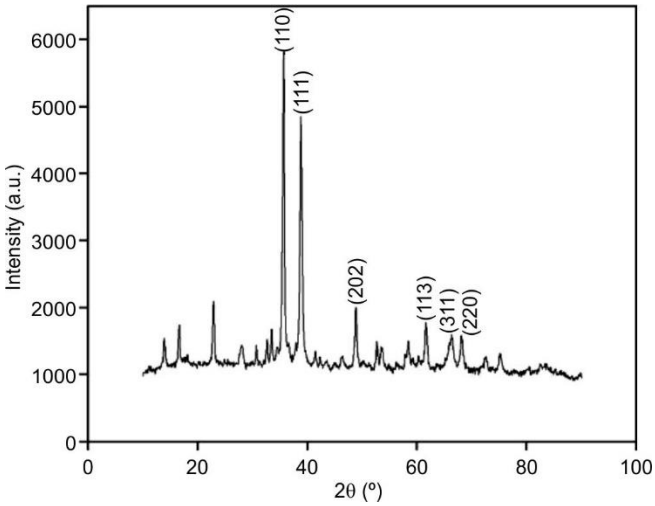

Fig. 5. X-Ray diffraction pattern of COEC nanoparticle

The TEM analysis showed that the nanoparticles ranged in size from 10 to 70 nm, predominantly exhibiting rod-like shapes with occasional spherical forms. The SAED pattern (Fig. 6d) displayed distinct bright concentric rings, confirming the polycrystalline nature of the particles. The calculated interplanar *d*-spacing values for COEC (6.69, 7.35 and 7.36 nm) were consistent with reported values for polycrystalline CuO nanoparticles [37,38]. The relatively larger particle size observed for COEC can be attributed to the presence of chitosan, whose high viscosity promotes increased pore size and particle growth. Similar observations have been reported by Zhang *et al.* [39], where higher chitosan concentration led to increased viscosity and consequently larger particle sizes.

Viscosity index (VI) values: Table-3 displays the viscosity index (VI) values of the base oil blended with polymer/COEC nanocomposites, which demonstrate better performance than the pure polymer (0%). As the amount of polymer/COEC composites in the base oil increases, the VI values gradually increase as well. Copolymer/nanocomposites work better as viscosity modifiers than homopolymer/nanocomposite, as evidenced by the formulation containing 5% additive (P-2D) of copolymer/nanocomposites showing the most significant enhancement in VI compared to the other blends among the two polymers. This improvement is explained by the fact that when the additive concentration rises, a larger volume of polymer micelles forms in the lubricant. Moreover, the presence of nanoparticles encourages polymer chains to separate inside the matrix, increasing the volume of the composite as a whole. The viscosity index of lubricant eventually increases as a result of this increase in the effective volume of dispersed units inside the solution [40].

Pour point depressant (PPD): The performance of polymer/COEC nanocomposite additives was evaluated for their effectiveness as pour point depressants (PPDs) in base oil. Table-4 shows the experimentally determined pour points of lubricants mixed with polymers at concentrations ranging from 1% to 5% (w/w). According to the findings, the copolymer/COEC nanocomposite outperformed the homopolymer/COEC nanocomposite in terms of PPD performance [41]. These produced polymers demonstrated a considerable increase in effectiveness with polymer concentrations up to

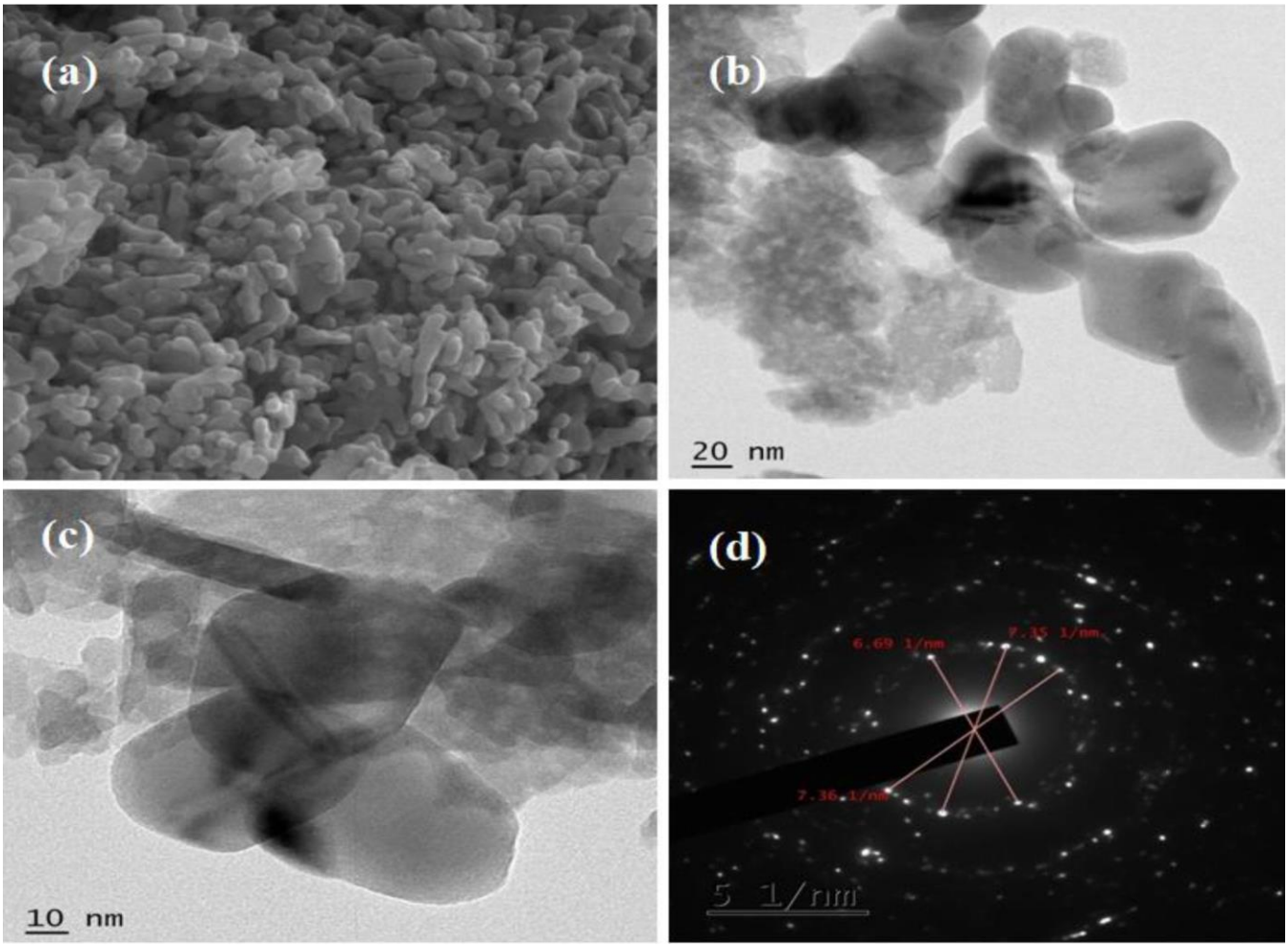

Fig. 6. (a) SEM, (b,c) TEM and (d) SAED images of COEC nanoparticle

TABLE-3
VISCOSITY INDEX OF LUBE OIL BLENDED WITH ADDITIVES (HOMOPOLYMER–COEC AND COPOLYMER–COEC NANOCOMPOSITE) AT VARYING CONCENTRATION LEVELS

Sample code	Homopolymer–COEC nanocomposite						Copolymer–COEC nanocomposite					
	0%	1%	2%	3%	4%	5%	0%	1%	2%	3%	4%	5%
P-1/P-2	83	87	91	98	103	108	83	89	93	99	105	112
P-1A/P-2A	83	95	102	112	116	119	83	95	104	109	115	119
P-1B/P-2B	83	96	107	114	120	124	83	98	107	115	123	126
P-1C/P-2C	83	98	112	120	124	129	83	100	113	122	128	132
P-1D/P-2D	83	100	114	124	127	134	83	102	118	126	134	138

P-1/P-2: homopolymer/copolymer (homo/copo); P-1A/P-2A: homo/copo/0.01% COEC composite; P-1B/P-2B: homo/copo/0.02% COEC composite; P-1C/P-2C: homo/copo/0.03% COEC composite; P-1D/P-2D: homo/copo/0.04% COEC composite

TABLE-4
POUR POINT VALUES (ºC) OF BASE OIL BLENDED WITH HOMOPOLYMER–COEC AND COPOLYMER–COEC NANOCOMPOSITE ADDITIVES AT VARYING CONCENTRATIONS (0-5% w/w) FOR DIFFERENT SAMPLE CODES

Sample code	Homopolymer–COEC nanocomposite						Copolymer–COEC nanocomposite					
	0%	1%	2%	3%	4%	5%	0%	1%	2%	3%	4%	5%
P-1/P-2	-7	-9	-12	-14	-16	-17	-7	-10	-13	-15	-16	-18
P-1A/P-2A	-7	-10	-12	-13	-17	-18	-7	-12	-12	-15	-17	-20
P-1B/P-2B	-7	-11	-14	-16	-20	-21	-7	-12	-14	-16	-18	-22
P-1C/P-2C	-7	-12	-15	-18	-21	-22	-7	-13	-15	-15	-19	-23
P-1D/P-2D	-7	-13	-15	-16	-19	-23	-7	-14	-16	-17	-19	-24

P-1/P-2: homopolymer/copolymer (homo/copo); P-1A/P-2A: homo/copo/0.01% COEC composite; P-1B/P-2B: homo/copo/0.02% COEC composite; P-1C/P-2C: homo/copo/0.03% COEC composite; P-1D/P-2D: homo/copo/0.04% COEC composite

TABLE-5
ANTIWEAR PROPERTY IN TERMS OF WEAR SCAR DIAMETER (WSD, mm) VALUES OF DIFFERENT LUBRICANT COMPOSITION OF HOMOPOLYMER-COEC AND COPOLYMER–COEC NANOCOMPOSITE WSD OF LUBE OIL (mm) AT DIFFERENT ADDITIVE CONCENTRATION

Sample code	Homopolymer–COEC nanocomposite						Copolymer–COEC nanocomposite					
	0%	1%	2%	3%	4%	5%	0%	1%	2%	3%	4%	5%
P-1/P-2	1.117	1.069	1.054	1.038	1.021	1.010	1.117	1.055	1.042	1.031	1.013	1.998
P-1A/P-2A	1.117	1.005	0.951	0.911	0.900	0.875	1.117	1.983	0.950	0.917	0.895	0.862
P-1B/P-2B	1.117	1.000	0.921	0.885	0.852	0.830	1.117	1.948	0.915	0.870	0.840	0.800
P-1C/P-2C	1.117	0.962	0.910	0.850	0.821	0.805	1.117	0.920	0.872	0.833	0.800	0.783
P-1D/P-2D	1.117	0.950	0.872	0.839	0.805	0.790	1.117	0.900	0.856	0.812	0.770	0.750

P-1/P-2: homopolymer/copolymer (homo/copo); P-1A/P-2A: homo/copo/0.01% COEC composite; P-1B/P-2B: homo/copo/0.02% COEC composite; P-1C/P-2C: homo/copo/0.03% COEC composite; P-1D/P-2D: homo/copo/0.04% COEC composite

5% in terms of pour point reduction. This implies that the base oil's paraffinic wax interacts with the polymers, causing the paraffinic wax crystals to shrink in size. The P-2D copolymer/COEC nanocomposite in particular showed improved PPD performance, which was probably caused by its greater polydispersity index (PDI). These findings is in align with the previously finding reports [42].

Anti-wear property: Using an FBWT device, the anti-wear and frictional properties of the lubricant formulation which was created by mixing the polymers in SN150 base oil were assessed under an applied load of 392 N, as indicated in Table-5. The anti-wear effectiveness of lubricant was enhanced by adding polymer/COEC nanocomposites, as seen by the blended samples' lower WSD values. P-2D of the copolymer/COEC nanocomposite at 5% concentration demonstrated the most noticeable decrease in WSD values among all evaluated polymers. This shows that between the two metal contact surfaces, the lubricant forms a strong protective layer. The enhanced performance is likely due to the higher content of polar side chains in olive oil, particularly ester carbonyl groups. These functional groups facilitate both chemical and physical interactions with metal surfaces in the contact zone, thereby strengthening the protective film formed by the additive molecules.

Conclusion

The outcomes of this work revealed that the synthesised *Elsholtzia blanda*-chitosan-mediated copper oxide nanoparticles (COEC) nanoparticles can effectively serve as filler materials in polymer composites. Their evaluation as lubricant additives showed that copolymer/COEC nanocomposites outperformed the homopolymer counterparts, acting as more effective viscosity modifiers, pour point depressants and anti-wear agents. These findings demonstrate the potential of this approach for developing multifunctional additive systems for high-performance lubricating oils.

CONFLICT OF INTEREST

The authors declare that there is no conflict of interests regarding the publication of this article.

DECLARATION OF AI-ASSISTED TECHNOLOGIES

During the preparation of this manuscript, the authors used an AI-assisted tool(s) to improve the language. The authors reviewed and edited the content and take full responsibility for the published work.

REFERENCES

1. J. Li, T. Ren, H. Liu, D. Wang and W. Liu, *Wear*, **246**, 130 (2000); https://doi.org/10.1016/S0043-1648(00)00500-7
2. H. Jianqiang, Z. Huanqin, W. Li, W. Xianyong, J. Feng and Z. Zhiming, *Wear*, **259**, 519 (2005); https://doi.org/10.1016/j.wear.2005.02.116
3. I.E. Uflyand, V.A. Zhinzhilo and V.E. Burlakova, *Friction*, **7**, 93 (2019); https://doi.org/10.1007/s40544-019-0261-y
4. B. Zhmud and B. Pasalskiy, *Lubricants*, **1**, 95 (2013); https://doi.org/10.3390/lubricants1040095
5. Deepika, *SN Appl. Sci.*, **2**, 1128 (2020); https://doi.org/10.1007/s42452-020-2916-8
6. T. Li, X. Chen, J. Wang, L. Zhang, X. Wei, L. Zhao and M. Ma, *IOP Conf. Ser. Earth Environ. Sci.*, **680**, 012084 (2021); https://doi.org/10.1088/1755-1315/680/1/012084
7. W. Brostow, M. Dutta, J.R. de Souza, P. Rusek, A.M. de Medeiros and E.N. Ito, *Express Polym. Lett.*, **4**, 570 (2010); https://doi.org/10.3144/expresspolymlett.2010.71
8. L. Sun, J. Zhou, Z. Zhang and H. Dang, *Wear*, **256**, 176 (2004); https://doi.org/10.1016/S0043-1648(03)00386-7
9. L. Rapoport, V. Leshchinsky, I. Lapsker, O. Nepomnyashchy, Y. Volovik, M. Lvovsky, R. Popovitz-Biro, Y. Feldman and R. Tenne, *Wear*, **255**, 785 (2003); https://doi.org/10.1016/S0043-1648(03)00044-9
10. L. Kong, J. Sun and Y. Bao, *RSC Adv.*, **7**, 12599 (2017); https://doi.org/10.1039/C6RA28243A
11. J. Zhou, J. Yang, Z. Zhang, W. Liu and Q. Xue, *Mater. Res. Bull.*, **34**, 1361 (1999); https://doi.org/10.1016/S0025-5408(99)00150-6
12. S. Chen, W. Liu and L. Yu, *Wear*, **218**, 153 (1998); https://doi.org/10.1016/S0043-1648(98)00220-8
13. W. Liu and S. Chen, *Wear*, **238**, 120 (2000); https://doi.org/10.1016/S0043-1648(99)00344-0
14. Q. Xue, W. Liu and Z. Zhang, *Wear*, **213**, 29 (1997); https://doi.org/10.1016/S0043-1648(97)00200-7
15. Z.S. Hu, R. Lai, F. Lou, L.G. Wang, Z.L. Chen, G.X. Chen and J.X. Dong, *Wear*, **252**, 370 (2002); https://doi.org/10.1016/S0043-1648(01)00862-6
16. Q. Sunqing, D. Junxiu and C. Guoxu, *Wear*, **230**, 35 (1999); https://doi.org/10.1016/S0043-1648(99)00084-8
17. H.D. Huang, J.P. Tu, L.P. Gan and C.Z. Li, *Wear*, **261**, 140 (2006); https://doi.org/10.1016/j.wear.2005.09.010
18. T. Zou, J. Tu, H. Huang, D. Lai, L. Zhang and D. He, *Adv. Eng. Mater.*, **8**, 289 (2006); https://doi.org/10.1002/adem.200500218
19. H.D. Huang, J.P. Tu, T.Z. Zou, L.L. Zhang and D.N. He, *Tribol. Lett.*, **20**, 247 (2005); https://doi.org/10.1007/s11249-005-8552-z
20. W.X. Chen, J.P. Tu, Z.D. Xu, R. Tenne, R. Rosenstveig, W.L. Chen and H.Y. Gan, *Adv. Eng. Mater.*, **4**, 686 (2002); https://doi.org/10.1002/1527-2648(20020916)4:9<686::AID-ADEM686>3.0.CO; 2-I

21. Y.Y. Wu, W.C. Tsui and T.C. Liu, *Wear*, **262**, 819 (2007); https://doi.org/10.1016/j.wear.2006.08.021
22. C.X. Gu, G.J. Zhu, L. Li, X.Y. Tian and G.Y. Zhu, *J. Mar. Sci. Appl.*, **8**, 71 (2009); https://doi.org/10.1007/s11804-009-8008-1
23. S. Salem, H. Abuzied, W.M. Sadek, K. Sakr and T. Elmeligy, *J. Eng. Appl. Sci.*, **72**, 266 (2025); https://doi.org/10.1186/s44147-025-00855-x
24. J. Zhou, Z. Wu, Z. Zhang, W. Liu and Q. Xue, *Tribol. Lett.*, **8**, 213 (2000); https://doi.org/10.1023/A:1019151721801
25. B. Li, X. Wang, W. Liu and Q. Xue, *Tribol. Lett.*, **22**, 79 (2006); https://doi.org/10.1007/s11249-005-9002-7.
26. Y.D. Zhang, J.S. Yan, L.G. Yu and P.Y. Zhang, *Tribol. Lett.*, **37**, 203 (2010); https://doi.org/10.1007/s11249-009-9515-6
27. P. Ghosh and M. Upadhyay, *J. Polym. Res.*, **23**, 100 (2016); https://doi.org/10.1007/s10965-016-0990-9
28. P. Ghosh, S. Talukder, M. Upadhyay and T. Das, *J. Sci. Ind. Res.*, **75**, 420 (2016).
29. T. Jayaramudu, K. Varaprasad, R.D. Pyarasani, K.K. Reddy, K.D. Kumar, A. Akbari-Fakhrabadi, R.V. Mangalaraja and J. Amalraj, *Int. J. Biol. Macromol.*, **128**, 499 (2019); https://doi.org/10.1016/j.ijbiomac.2019.01.145
30. A. Roselyn Maheo, B. Scholastica Mary Vithiya, T. Augustine Arul Prasad, P. Tamizhdurai and V.L. Mangesh, *Arab. J. Chem.*, **15**, 103661 (2022); https://doi.org/10.1016/j.arabjc.2021.103661
31. K. Dey, G. Karmakar, M. Upadhyay and P. Ghosh, *Sci. Rep.*, **10**, 19151 (2020); https://doi.org/10.1038/s41598-020-76246-4
32. D.K. Saha and P. Ghosh, *J. Macromol. Sci. Part A Pure Appl. Chem.*, **55**, 384 (2018); https://doi.org/10.1080/10601325.2018.1444419
33. S. Tanveer and R. Prasad, *Indian J. Chem. Technol.*, **13**, 398 (2006).
34. G. Karmakar and P. Ghosh, *ACS Sustain. Chem. Eng.*, **3**, 19 (2015); https://doi.org/10.1021/sc500685r
35. K. Dey, G. Karmakar, M. Upadhyay and P. Ghosh, *Sci. Rep.*, **10**, 19151 (2020); https://doi.org/10.1038/s41598-020-76246-4
36. L.Y. Maroufi and M. Ghorbani, *Int. J. Biol. Macromol.*, **177**, 485 (2021); https://doi.org/10.1016/j.ijbiomac.2021.02.113
37. K. Velsankar, S. Suganya, P. Muthumari, S. Mohandoss and S. Sudhahar, *J. Environ. Chem. Eng.*, **9**, 106299 (2021); https://doi.org/10.1016/j.jece.2021.106299
38. A.A. Mohamed, M. Abu-elghait, N.E. Ahmed, S.S. Salem and S.S. Salem, *Biol. Trace Elem. Res.*, **199**, 2788 (2021); https://doi.org/10.1007/s12011-020-02369-4
39. S. Zhang and K. Kawakami, *Int. J. Pharm.*, **397**, 211 (2010); https://doi.org/10.1016/j.ijpharm.2010.07.007
40. P. Ghosh and M. Das, *J. Chem. Eng. Data*, **58**, 510 (2013); https://doi.org/10.1021/je3008793
41. A.A.A. Azim, A.M. Nassar, N.S. Ahmed and R.S. Kamal, *Petrol. Sci. Technol.*, **24**, 37 (2006); https://doi.org/10.1081/LFT-200041129.
42. P. Ghosh, T. Das, D. Nandi, G. Karmakar and A. Mandal, *Int. J. Polym. Mater.*, **59**, 1008 (2010); https://doi.org/10.1080/00914037.2010.504156